Coronene Encapsulation in Single-Walled Carbon Nanotubes: Stacked Columns, Peapods, and Nanoribbons

Ilya V. Anoshkin,*[a] Alexandr V. Talyzin,*[b] Albert G. Nasibulin,[a, e] Arkady V. Krasheninnikov,[c] Hua Jiang,[a] Risto M. Nieminen,[d] and Esko I. Kauppinen[a]

Encapsulation of coronene inside single-walled carbon nanotubes (SWNTs) was studied under various conditions. Under high vacuum, two main types of molecular encapsulation were observed by using transmission electron microscopy: coronene dimers and molecular stacking columns perpendicular or tilted (45–60°) with regard to the axis of the SWNTs. A relatively small number of short nanoribbons or polymerized coronene molecular chains were observed. However, experiments performed under an argon atmosphere (0.17 MPa) revealed reac-

tions between the coronene molecules and the formation of hydrogen-terminated graphene nanoribbons. It was also observed that the morphology of the encapsulated products depend on the diameter of the SWNTs. The experimental results are explained by using density functional theory calculations through the energies of the coronene molecules inside the SWNTs, which depend on the orientation of the molecules and the diameter of the tubes.

1. Introduction

Graphene nanoribbons (GNRs) are of great interest for various applications due to their unique electronic properties.[1–7] GNRs can be synthesized by using a variety of methods, for example, by unzipping carbon nanotubes,[1,4,8–13] cutting two-dimensional (2D) graphene sheets by electron or ion beams,[14,15] and by template growth.[3,16] One of the most promising directions in this field is the bottom-to-top approach, which suggests the use of molecular blocks (typically some hydrocarbons) for the construction of GNRs with variable widths and edge types.[3,14–16] This approach was used in our recent study to make hydrogen-terminated graphene nanoribbons encapsulated inside single-walled carbon nanotubes (SWNTs).[17] We demonstrated a very simple and efficient method for the synthesis of hydrogen-terminated graphene nanoribbons encapsulated

in SWNTs by using thermally induced fusion of the molecular precursors: coronene and perylene.[17] The nanoribbons exhibited certain distinct signatures by photoluminescence spectroscopy.[18] Notably, sulfur-terminated nanoribbons were recently synthesized inside SWNTs by using a different approach: disintegrating precursor molecules on atomic species by using an electron beam or high-temperature pyrolysis.[19,20] A number of theoretical studies on the encapsulation of GNRs into SWNTs has been recently published.[21–26]

Coronene is a large polycyclic aromatic hydrocarbon (PAH) molecule easily soluble and stable upon evaporation.[27,28] It was considered in many theoretical studies as a model of nanographene terminated by hydrogen.[29–31] It is well known that annealing coronene at certain temperatures leads to a fusion reaction with the formation of a coronene dimer, that is, dicoronylene.[32,33] Planar fusion of several coronene molecules was suggested as a road to the formation of progressively larger graphene flakes.[28] Carbon nanotubes were used as a one-dimensional (1D) reactor to provide edge-to-edge alignment of molecules required for the fusion reaction into graphene nanoribbons.[17] However, the mechanism of coronene polymerization and nanoribbon formation is not yet clear, and studies of the chemical reactions both in a confined space (1D or 2D) and in a free molecular phase are of great interest.[30,34]

Encapsulation of coronene and dicoronylene in SWNTs was previously reported by Okazaki et al., and the formation of nanoribbons was not observed.[35] Experimental and theoretical studies showed that encapsulated coronene molecules can be packed into columns with parallel graphite-like stacking in the inner space of SWNTs.[35,36] In contrast, parallel stacking of coronene molecules was not observed in our previous experiments even if the temperature of encapsulation was lowered below the melting point of coronene (down to 420 °C).[17] Detailed

[a] Dr. I. V. Anoshkin,+ Prof. A. G. Nasibulin, H. Jiang, Prof. E. I. Kauppinen
NanoMaterials Group, Department of Applied Physics
Aalto University, P.O. Box 15100
00076 Aalto, Espoo (Finland)
E-mail: ilya.anoshkin@aalto.fi

[b] Dr. A. V. Talyzin+
Umeå University, Department of Physics
90187 Umeå (Sweden)
E-mail: alexandr.talyzin@physics.umu.se

[c] Dr. A. V. Krasheninnikov
Department of Applied Physics, Aalto University,
P.O. Box 1100, 00076 Aalto (Finland)

[d] Prof. R. M. Nieminen
Aalto University School of Science
P.O. Box 1100, 00076 Aalto (Finland)

[e] Prof. A. G. Nasibulin
Skolkovo Institute of Science and Technology
100 Novaya st., Skolkovo, 143025 (Russia)

[+] These authors contributed equally to this work

analysis of the synthesis conditions used for the encapsulation of coronene in these two studies showed one significant difference: stacking columns of coronene molecules and coronene dimers were obtained if encapsulation was performed under vacuum conditions,[24,35,37] whereas our experiments were performed under an argon atmosphere at pressures slightly above ambient (≈ 0.17 MPa).[17] Notably, recent attempts to synthesize GNR@SWNTs by using coronene and perylene precursors have also been performed by using traditional vacuum conditions encapsulation.[37–39] Our new experiments demonstrate that the selection of the synthesis conditions is crucial and allows the control of the type of coronene encapsulation in SWNTs. Herein, we demonstrate that the product encapsulated inside the SWNTs can be altered from coronene peapods and columns with parallel stacking to polymerized coronene in the form of GNRs depending on the conditions.

Experimental Section

SWNTs were synthesized by an aerosol chemical vapor deposition method based on CO disproportionation on iron nanoparticles produced by ferrocene vapor decomposition at $1000\,°C$ as described elsewhere.[40,41] A thin film of SWNTs was transferred onto a fused silica plate, and the nanotubes were opened through oxidation in air ($390\,°C$, 30 min) and washed with aqueous HCl to remove any residual catalyst. The SWNT films were sealed in Pyrex tubes with coronene powder (5–7 mg; 97%, Sigma–Aldrich) under high vacuum (≈ 1 Pa). Annealing was performed for 22–24 h at $440\,°C$. The treatment temperature was just above the melting point of coronene ($438\,°C$) and below the temperatures for the dimerization and fusion reactions of coronene, which occur in pure coronene vapor above $520\,°C$.[42] Notably, the coronene dimerization reaction is assisted by residual oxygen and occurs at lower temperatures under lower vacuum (≈ 10 Pa). Residual coronene was removed by careful washing with toluene, whereas some dicoronylene impurities were likely preserved in the studied samples.

High-resolution transmission electron microscopy (TEM) images were obtained with a double Cs-corrected JEOL JEM-2200FS microscope.[43] To minimize the destructive influence of electron irradiation, all samples were analyzed at an acceleration voltage of 80 kV with the shortest possible electron illumination time. Raman spectra were recorded by using a Renishaw spectrometer equipped with a 514 nm laser.

2. Results and Discussion

The Raman spectra recorded from samples of SWNTs exposed to coronene vapor under vacuum conditions confirmed that some coronene products precipitated in the samples and that they were not removed even after very careful washing with toluene. However, only detailed high-resolution TEM imaging allowed the geometry of the encapsulated coronene to be revealed and the presence/absence of coronene polymerization. As shown in our earlier study, the Raman spectra of annealed coronene powders remained almost unchanged even if the reaction clearly went beyond the formation of dimers into some complex oligomer mixtures.[42] This was also confirmed recently by using theoretical simulations of Raman spectra from coronene polymers of different lengths.[37] The Raman coronene

features in the samples obtained under an argon atmosphere and prepared under vacuum conditions appeared to be identical (Figure 1; see also ref. [44]). Figure 1 shows no shift in the radial breathing modes and a set of additional bands due to the encapsulation of coronene. The low intensity of these additional bands is consistent with the high purity of the sample
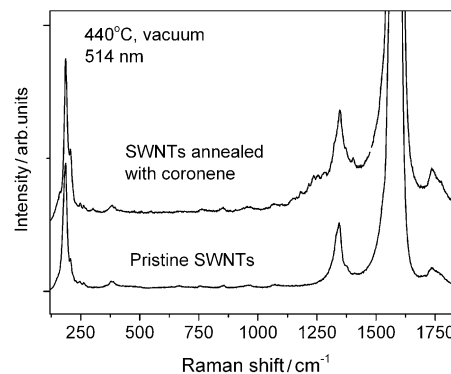

Figure 1. Raman spectra (514 nm laser) recorded from pristine SWNTs and from the sample annealed with coronene under vacuum (at $440\,°C$). Coronene-related bands were found in the region around $1200–1450\ cm^{-1}$.

and the absence of significant contamination by residual (not encapsulated) coronene or dicoronylene. However, TEM investigation of the samples synthesized under vacuum conditions clearly demonstrated the difference: the nanotubes appeared to be filled by coronene mainly in a molecular form, that is, GNRs were not obtained as a main product of encapsulation by using the same temperatures as those in ref. [17].

Columnar stacking of the coronene molecules was observed as a common type of encapsulation in the vacuum-synthesized samples, which is in good agreement with the data obtained by Okazaki et al.[35] (Figure 2). The stacked coronene molecules seem to be rather unstable under the electron beam. Amorphization of the columns occurs after several minutes during the common focusing procedure with an electron energy of 80 kV and with an electron beam with an intensity of about $2.3 \times 10^4\ e^-\,Å^{-2}\,s^{-1}$. Notably, for the successful observation of the col-
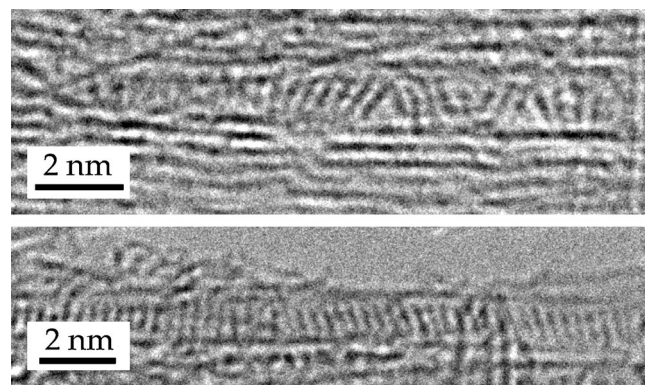

Figure 2. TEM images showing columnar stacking of the coronene molecules inside the SWNTs after filling at $440\,°C$ under vacuum. The diameters of the SWNT are 1.48 nm (top) and 1.42 nm (bottom).

umnar stacking of coronene, techniques with electron illumination doses as low as possible should be used. The distance between the coronene molecules measured from Figure S1 (0.317 nm, see the Supporting Information) correlated within 5% to the interlayer distance typically observed in graphite (0.335 nm). The images shown in Figure 2 confirm our initial hypothesis that vacuum conditions are required for the crystallization of coronene molecules in a parallel stacking mode inside the SWNTs. Detailed study of these samples also revealed some coronene structures other than columnar and the dependence of their geometry on the diameter of the SWNTs.

The SWNTs used for this study had a broad distribution of diameters (1.1–1.9 nm), which clearly affected the encapsulation of coronene. The stacking encapsulation requires a certain match of the size of the coronene molecule with the diameter of the nanotube. If the diameter of the nanotube is slightly smaller than an ideal diameter for filling, the plane size of the coronene molecule appears to be too large for the formation of a 1D crystal with the orientation of the molecular plane perpendicular to the axis of the SWNT. As a result, a structure with coronene molecules oriented with a tilt to the nanotube walls is observed. The packing structure is maintained (Figure 2), but with mismatch angles up to 60°. Another type of coronene encapsulation is shown in Figure 3 and can be termed coronene peapods similar to fullerene peapods.

Figure 3 shows a peapod-type of encapsulation of some objects similar to fullerenes in the size and contrast. However, contamination of our samples with fullerenes can be certainly ruled out. Also, the size of the encapsulated molecules was smaller (0.45–0.61 nm) than the size of fullerene C_{60} molecules (0.7 nm). Unambiguous assignment of these objects to coronene is possible due to images that show the overlap of individual molecules inside the SWNTs (partial stacking of planar molecules observed almost perpendicular to the planes). This type of overlap is not possible for spherical fullerene molecules inside nanotubes of a given diameter due to geometrical limitations (see Figures S3 and S4). It is very likely that the coronene molecules (or dimers, trimers, etc.) could be oriented perpendicular to the TEM electron beam. The images in Figure 3b

show a region in which molecules are clearly separated from each other and a region in which they are packed together into some kind of polymeric chain (Figure S2). These structures can be considered as precursors or intermediates of GNR formation.[17]

The coronene molecules are moving inside the SWNTs, as demonstrated by a set of images collected from the same spot with short time intervals (see the movie in the Supporting Information). Figure 4 shows a time sequence of TEM images
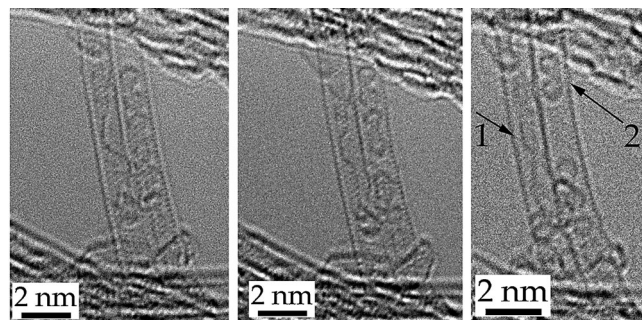

Figure 4. Time sequence TEM images showing two nanotubes with a diameter of 1.3 nm, one filled with a nanoribbon wiggling under the electron beam (see arrow 1) and the second with peapod-type encapsulation (see arrow 2 showing coronene dimer molecule).

with two nanotubes: one of them with peapod-like encapsulation of coronene molecules and a second with encapsulated nanoribbon. The set of images clearly shows how the coronene molecules move inside the nanotube space; both single molecules and dimers can be recognized. The dimer (dicoronylene) molecules seem to be stable under the electron beam, and their motion inside the nanotube was observed in a long set of about 15 images without further polymerization or attachment to the walls. The overall time of electron illumination for the sample area was 6 min with an intensity of about $8.3 \times 10^6 \, e^- \, Å^{-2}$ and no noticeable nanotube damage was observed.

The neighboring nanotube (Figure 4, arrow 1) at the same time demonstrates a GNR, which experiences wave-like oscilla-
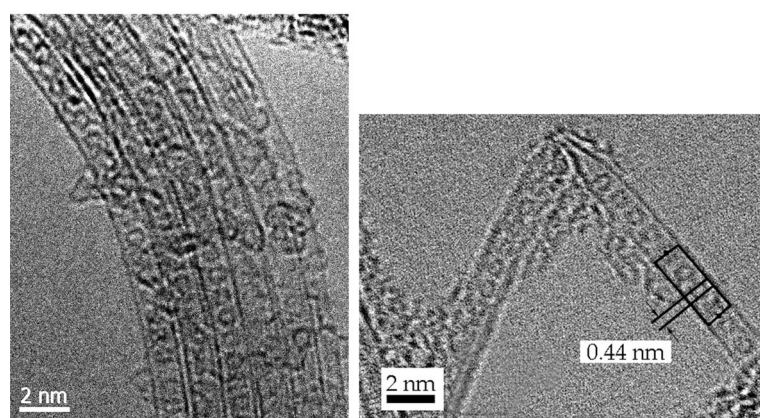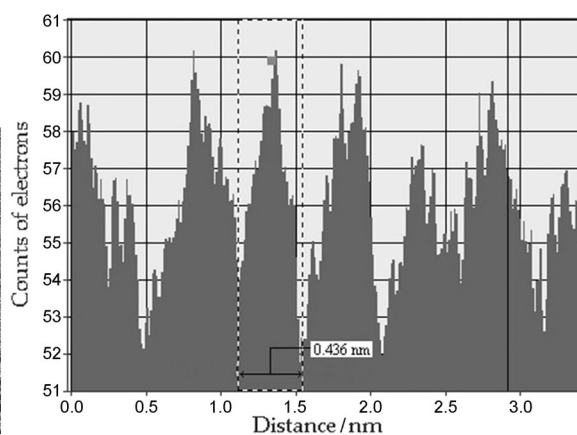

Figure 3. Coronene peapods synthesized under vacuum at 440 °C. a), b) TEM images, c) profile of b) in which the size of the individual molecules is in the range from 0.45 to 0.61 nm; the diameter of the SWNTs is around 1.6 nm.

tions and bending under the electron beam. The images also show the edge view for this nanoribbon. The end of the nanoribbon seems to be attached to the internal side of the SWNT, which allows clear observation of variations in the orientation of the nanoribbon, wave-like motion, and bending under the electron beam to be observed clearly. The images shown in Figure 4 unambiguously prove that the observed object is, indeed, a GNR and not, for example, an inner nanotube.

As noted above, only very few nanoribbons were found in the vacuum-synthesized samples, whereas synthesis at similar temperatures (440–470 °C) resulted in almost 100% filling of the SWNTs with GNRs if the reaction was performed under an argon atmosphere.[17] Theoretical simulations showed that argon inside the SWNTs makes some difference in the encapsulation of the molecules.[44] Argon as an inert gas is unlikely to participate in the polymerization reaction of coronene directly. However, the experimental results demonstrate that the presence of argon hinders the stacking geometry of encapsulation. A possible role of argon is to slow down the diffusion of the coronene molecules into the inner space of the nanotube, which provides conditions for the edge-to-edge geometry required for the polymerization of coronene with the formation of hydrogen-terminated GNRs. If the nanotubes are also sufficiently wide for encapsulation of argon, the coronene molecules would need to penetrate into the argon-filled nanotubes, and at the same time, the argon atoms would escape from the cavities of the SWNTs. This would change the reaction conditions inside the nanotube dramatically. Notably, another famous example in which an inert gas provided conditions for assembling simple carbon species into geometrically complex molecules is the arc synthesis of fullerenes under an atmosphere of argon or helium.[45] The synthesis of fullerenes does not occur in the arc under vacuum conditions, whereas the presence of the inert gases helps the reaction.

An important parameter that affects the encapsulation product is the size matching between the initial precursor molecule and the diameter of the SWNT. The diameter of a coronene molecule is about 0.7 nm. Considering a van der Waals distance of about 0.35 nm, the ideal diameter for coronene encapsulation should be about 1.4 nm. Statistical processing of images with various types of encapsulations showed that parallel stacked coronene columns were mostly formed in SWNTs with outer diameters between 1.1 and 1.4 nm, whereas GNRs were found most frequently in SWNTs with diameters of 1.3–1.8 nm. Separate molecules and coronene dimers were observed in all tubes with diameters over 1.0 nm without any SWNT diameter selectivity. The small diameter tubes (≤ 1 nm) did not show coronene encapsulation.

SWNTs with larger diameters cannot provide an orientation effect, and the morphology of the product resulting from coronene encapsulation and fusion becomes rather irregular. In the SWNTs with $d > 2.0$ nm, only zigzag-shaped GNRs and geometrically irregular debris-like products were observed (Figure S3). Notably, similar observations were recently reported for sulfur-terminated nanoribbons that showed clear correlation with the diameter of the SWNTs, and the nanoribbons were not observed inside nanotubes with diameters over about 2 nm.[20]

The effects of coronene encapsulation in SWNTs were also studied theoretically by using spin-polarized density functional theory (DFT) calculations with a nonlocal exchange and correlations functional,[46] which is capable of describing both short-range covalent bonding and long-range van der Waals type interactions between the nanotubes and the coronene molecules inside of them, implemented in the plane-wave basis-set VASP[47] code. Even though this approach does not fully account for many-body effects, which may be particularly important in nanoscale systems with complex geometry,[48,49] the comparison[50] of the results for 2D systems obtained with that functional and within the random-phase approximation indicates that this functional correctly reproduces all of the trends, even though the binding energy is overestimated. In any case, the accuracy of our approach is sufficient to provide at least qualitative information on the behavior of the system. The projector augmented wave potentials[51] was employed to describe the core electrons The nonlocal term in the van der Waals density functional was evaluated by using the adaptive real-space approach.[52] The total energies of the system were converged within 0.0001 eV atom^{-1} with regard to the number of K points and the plane-wave cut-off energy.

The three characteristic positions of the coronene molecules inside the nanotube were calculated: perpendicular, parallel, and tilted with regard to tube axis. Zigzag SWNTs with chiral indices of (15,0), (18,0), and (20,0) were considered. During energy optimization, all atoms were allowed to move without any constraints, except for the six central atoms in the coronene molecule, which fixed the orientation of the molecule.

For the (15.0) nanotubes with a diameter of 1.18 nm, all three positions of the coronene molecules were energetically unfavorable with respect to the isolated tube and the coronene molecule, so that the binding energy E_b (defined as the difference between the total energies of the composite systems and the isolated constituents) was positive (Figure 5). The lowest-energy configuration was a tilted position ($E_b = 0.8$ eV). The position along the axis was higher in energy and reached 2.2 eV, and the least energetically favorable configuration of the coronene molecules was perpendicular to the axis of the nanotube ($E_b = 10$ eV). All of these configurations gave rise to a local distortion of the nanotube. Thus, the absence of coronene molecules in tubes with a diameter less than 1.2 nm in the experimental TEM images very well correlates with the results of the calculations.

In contrast to the (15,0) nanotube, for the (18,0) tube with a diameter of 1.41 nm all three positions of the coronene molecules were energetically favorable. The most energetically favorable configuration was the tilted one ($E_b = -1.03$ eV).

The van der Waals binding energy for coronene molecules inside the nanotubes is shown as a function of angle in Figure 6. For a large-diameter (20,0) nanotube, the energy minimum corresponds to $\Theta = 90°$. For a smaller diameter (18,0) nanotube, the energy minimum corresponds to $\Theta = 60°$. For a small-diameter (15,0) nanotube, the minimum corresponds to smaller angles, but it is energetically unfavorable for the molecule to get inside. These results can be understood from geometrical considerations. As the simulations indicate, the
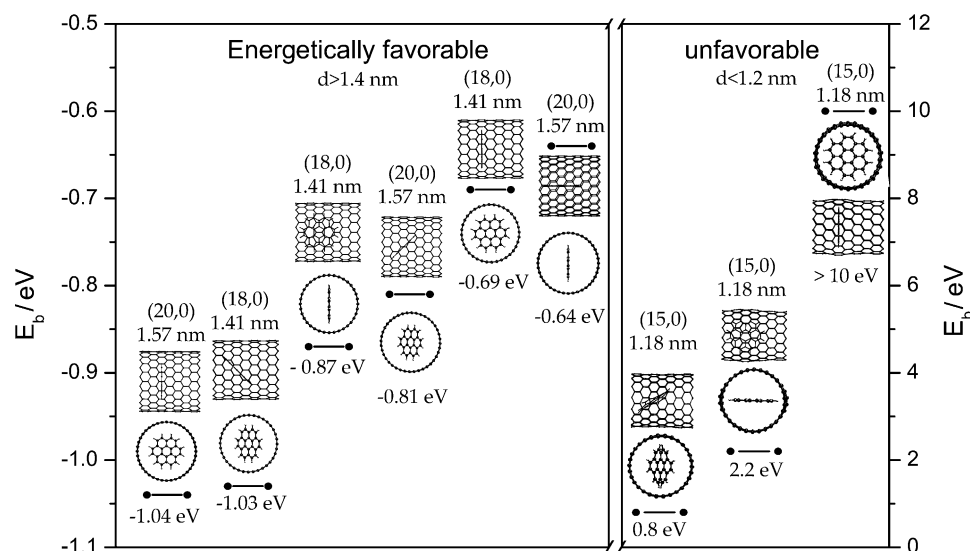
Figure 5. The results of DFT simulation of the binding energy (E_b) for the (15,0), (18,0), and (20,0) SWNTs with coronene molecules inside.
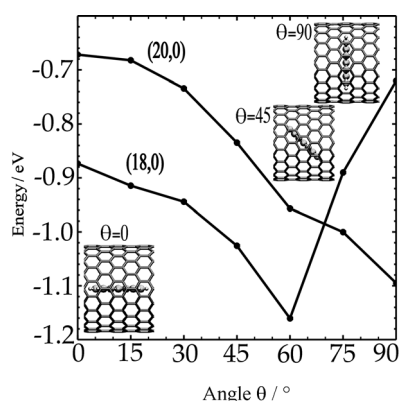

Figure 6. The binding energy for the isolated coronene molecule inside the (20,0) and (18,0) SWNTs as a function of tilting angle (Θ).

(under vacuum conditions), but it is also likely that it can form inside the SWNTs.

Summarizing the results presented in this study, encapsulation into SWNTs is traditionally performed under vacuum conditions with the assumption that the nanotubes must be empty to accommodate various molecules. However, our experiments revealed that filling nanotubes under an atmosphere of argon gas provides rather different conditions for encapsulation of planar molecules and results in different kinds of products if the molecules react with each other inside the nanotubes. It is clear that many other gases, including reactive ones such as hydrogen, can be used to modify the chemistry inside the carbon nanotubes.[38] The geometrical effect of argon for the encapsulation of molecules into SWNTs demonstrated in our study is likely to be found for other gases as well and may possibly lead to the synthesis of new materials by using reactions of molecules in a space not only confined by the walls of the nanotube but also by the pressure of various gases.

minimum energy separation between graphene and the perpendicular-oriented coronene molecule is 0.265 nm. The diameter of the (20,0) tube is 1.57 nm; then, the separation between the walls of the SWNT and the coronene molecule (oriented perpendicular to the tube axis) is 0.3 nm, which is larger than the optimum separation. To maximize the interaction, the molecule is perpendicular oriented. The (18,0) tube has a diameter of 1.41 nm. The separation of 0.23 nm is less than 0.265 nm and so the molecule will be rotated. The same effect should be valid for tubes with smaller diameters—the coronene molecules will be tilted.

Another factor that possibly contributes to the formation of stacking encapsulation is the reaction of coronene molecules under vacuum with the formation of dicoronylene. The dicoronylene molecule is too large to form stacking columns inside nanotubes and, therefore, it penetrates into the SWNTs only with the orientation of the long axis parallel to the axis of the nanotube. As demonstrated by Fujihara et al.,[37] dicoronylene can be encapsulated into nanotubes directly from the vapor

3. Conclusions

Exposure of opened SWNTs to coronene molecule vapors resulted in drastically different types of encapsulation depending on the conditions. Vacuum provides conditions for encapsulation of coronene into SWNTs in a predominantly molecular form. Two types of molecular encapsulation were observed in this study. The first type is when molecules are aligned parallel to each other to form column stacking, and the second is peapod-like with molecules moving inside the SWNTs, similar to fullerenes.

The results of DFT calculations are in agreement with the TEM observations and showed that the type of encapsulation depends on the diameter of the SWNT. The encapsulation of coronene is energetically unfavorable for SWNTs with diameters less than 1.2 nm, and the encapsulation of columns from tilted molecules is favorable for nanotubes with diameters of 1.3–1.6 nm. For larger tubes, the formation of overlapped structures and debris is favorable.

For SWNTs with diameters between 1.4 and 1.8 nm, the encapsulation of coronene in the presence of argon assists reactions between molecular edges and formation of graphene nanoribbon. It is very likely that many other reactions performed inside carbon nanotubes and the encapsulation of various molecules can be very strongly affected if performed under a certain pressure of various gases.

Acknowledgements

[1] D. V. Kosynkin, A. L. Higginbotham, A. Sinitskii, J. R. Lomeda, A. Dimiev, B. K. Price, J. M. Tour, *Nature* **2009**, *458*, 872.

[2] L. Y. Jiao, L. Zhang, X. R. Wang, G. Diankov, H. J. Dai, *Nature* **2009**, *458*, 877.

[3] J. M. Cai, P. Ruffieux, R. Jaafar, M. Bieri, T. Braun, S. Blankenburg, M. Muoth, A. P. Seitsonen, M. Saleh, X. L. Feng, K. Mullen, R. Fasel, *Nature* **2010**, *466*, 470.

[4] L. Y. Jiao, X. R. Wang, G. Diankov, H. L. Wang, H. J. Dai, *Nat. Nanotechnol.* **2010**, *5*, 321.

[5] T. Shimizu, J. Haruyama, D. C. Marcano, D. V. Kosinkin, J. M. Tour, K. Hirose, K. Suenaga, *Nat. Nanotechnol.* **2011**, *6*, 45.

[6] A. Hirsch, *Angew. Chem.* **2009**, *121*, 6718; *Angew. Chem. Int. Ed.* **2009**, *48*, 6594.

[7] K. A. Ritter, J. W. Lyding, *Nat. Mater.* **2009**, *8*, 235.

[8] D. V. Kosynkin, W. Lu, A. Sinitskii, G. Pera, Z. Z. Sun, J. M. Tour, *ACS Nano* **2011**, *5*, 968.

[9] A. Sinitskii, A. Dimiev, D. V. Kosynkin, J. M. Tour, *ACS Nano* **2010**, *4*, 5405.

[10] J. W. Bai, R. Cheng, F. X. Xiu, L. Liao, M. S. Wang, A. Shailos, K. L. Wang, Y. Huang, X. F. Duan, *Nat. Nanotechnol.* **2010**, *5*, 655.

[11] A. V. Talyzin, S. Luzan, I. V. Anoshkin, A. G. Nasibulin, H. Jiang, E. I. Kauppinen, V. M. Mikoushkin, V. V. Shnitov, D. E. Marchenko, D. Noreus, *ACS Nano* **2011**, *5*, 5132.

[12] C. H. Jin, H. P. Lan, L. M. Peng, K. Suenaga, S. Iijima, *Phys. Rev. Lett.* **2009**, *102*, 205501.

[13] M. C. Lemme, D. C. Bell, J. R. Williams, L. A. Stern, B. W. H. Baugher, P. Jarillo-Herrero, C. M. Marcus, *ACS Nano* **2009**, *3*, 2674.

[14] M. Treier, C. A. Pignedoli, T. Laino, R. Rieger, K. Mullen, D. Passerone, R. Fasel, *Nat. Chem.* **2011**, *3*, 61.

[15] I. Diez-Perez, Z. H. Li, J. Hihath, J. H. Li, C. Y. Zhang, X. M. Yang, L. Zang, Y. J. Dai, X. L. Feng, K. Muellen, N. J. Tao, *Nat. Commun.* **2010**, *1*, 1.

[16] M. Sprinkle, M. Ruan, Y. Hu, J. Hankinson, M. Rubio-Roy, B. Zhang, X. Wu, C. Berger, W. A. de Heer, *Nat. Nanotechnol.* **2010**, *5*, 727.

[17] A. V. Talyzin, I. V. Anoshkin, A. V. Krasheninnikov, R. M. Nieminen, A. G. Nasibulin, H. Jiang, E. I. Kauppinen, *Nano Lett.* **2011**, *11*, 4352.

[18] A. I. Chernov, P. V. Fedotov, A. V. Talyzin, I. S. Lopez, I. V. Anoshkin, A. G. Nasibulin, E. I. Kauppinen, E. D. Obraztsova, *ACS Nano* **2013**, *7*, 6346.

[19] A. Chuvilin, E. Bichoutskaia, M. C. Gimenez-Lopez, T. W. Chamberlain, G. A. Rance, N. Kuganathan, J. Biskupek, U. Kaiser, A. N. Khlobystov, *Nat. Mater.* **2011**, *10*, 687.

[20] T. W. Chamberlain, J. Biskupek, G. A. Rance, A. Chuvilin, T. J. Alexander, E. Bichoutskaia, U. Kaiser, A. N. Khlobystov, *ACS Nano* **2012**, *6*, 3943.

[21] Y. Y. Jiang, H. Li, Y. F. Li, H. Q. Yu, K. M. Liew, Y. Z. He, X. F. Liu, *ACS Nano* **2011**, *5*, 2126.

[22] I. V. Lebedeva, A. M. Popov, A. A. Knizhnik, A. N. Khlobystov, B. V. Potapkin, *Nanoscale* **2012**, *4*, 4522.

[23] H. Shen, K. Cheng, *Mol. Simul.* **2012**, *38*, 922.

[24] F. Furuhashi, K. Shintani, *AIP Adv.* **2013**, *3*, 092103.

[25] L. Z. Kou, C. Tang, T. Frauenheim, C. F. Chen, *J. Phys. Chem. Lett.* **2013**, *4*, 1328.

[26] A. L. de Aguiar, A. Saraiva-Souza, Z. Bullard, D. W. Maia, A. G. S. Filho, E. C. Girão, V. Meunier, *Phys. Chem. Chem. Phys.* **2014**, *16*, 3603.

[27] J. K. Fawcett, J. Trotter, *Proc. R. Soc. London Ser. A* **1966**, *289*, 366.

[28] A. V. Talyzin, S. M. Luzan, L. Leifer, S. Akhtar, J. Fetzer, F. Cataldo, Y. O. Tsybin, C. V. Tai, A. Dzwilewski, E. Moons, *J. Phys. Chem. C* **2011**, *115*, 13207.

[29] Y. Zhao, D. G. Truhlar, *J. Phys. Chem. C* **2008**, *112*, 4061.

[30] R. Podeszwa, *J. Chem. Phys.* **2010**, *132*, 044704.

[31] T. S. Totton, A. J. Misquitta, M. Kraft, *J. Phys. Chem. A* **2011**, *115*, 13684.

[32] M. Zander, W. Franke, *Chem. Ber. Recl.* **1958**, *91*, 2794.

[33] R. Goddard, M. W. Haenel, W. C. Herndon, C. Kruger, M. Zander, *J. Am. Chem. Soc.* **1995**, *117*, 30.

[34] F. Cataldo, O. Ursini, G. Angelini, S. Iglesias-Groth, *Fullerenes Nanotubes Carbon Nanostruct.* **2011**, *19*, 713.

[35] T. Okazaki, Y. Iizumi, S. Okubo, H. Kataura, Z. Liu, K. Suenaga, Y. Tahara, M. Yudasaka, S. Okada, S. Iijima, *Angew. Chem.* **2011**, *123*, 4955; *Angew. Chem. Int. Ed.* **2011**, *50*, 4853.

[36] B. Verberck, T. Okazaki, N. V. Tarakina, *Phys. Chem. Chem. Phys.* **2013**, *15*, 18108.

[37] M. Fujihara, Y. Miyata, R. Kitaura, Y. Nishimura, C. Camacho, Y. Irle, Y. Iizumi, T. Okazaki, H. Shinohara, *J. Phys. Chem. C* **2012**, *116*, 15141.

[38] B. Botka, M. E. Fustos, G. Klupp, D. Kocsis, E. Szekely, M. Utczas, B. Simandi, A. Botos, R. Hackl, K. Kamaras, *Phys. Status Solidi B* **2012**, *249*, 2432.

[39] B. Botka, M. E. Fustos, H. M. Tohati, K. Nemeth, Z. Szekrényes, G. Klupp, D. Kocsis, M. Utczas, E. Szekely, T. Váczi, T. Tarczay, R. Hackl, T. W. Chamberlain, A. N. Khlobystov, K. Kamaras, *Small* **2013** DOI: 10.1002/smll.201302613.

[40] A. Moisala, A. G. Nasibulin, D. P. Brown, H. Jiang, L. Khriachtchev, E. I. Kauppinen, *Chem. Eng. Sci.* **2006**, *61*, 4393.

[41] Y. Tian, M. Timmermans, S. Kivistö, A. Nasibulin, Z. Zhu, H. Jiang, O. Okhotnikov, E. Kauppinen, *Nano Res.* **2011**, *4*, 807.

[42] A. V. Talyzin, S. M. Luzan, K. Leifer, S. Akhtar, J. Fetzer, F. Cataldo, Y. O. Tsybin, C. W. Tai, A. Dzwilewski, E. Moons, *J. Phys. Chem. C* **2011**, *115*, 13207.

[43] H. Jiang, J. Ruokolainen, N. Young, T. Oikawa, A. G. Nasibulin, A. Kirkland, E. I. Kauppinen, *Micron* **2012**, *43*, 545.

[44] V. Chaban, *Chem. Phys. Lett.* **2010**, *500*, 35.

[45] W. Krätschmer, L. D. Lamb, K. Fostiropoulos, D. R. Huffman, *Nature* **1990**, *347*, 354.

[46] O. A. Vydrov, T. Van Voorhis, *J. Chem. Phys.* **2010**, *133*, 244103.

[47] G. Kresse, J. Furthmuller, *Phys. Rev. B* **1996**, *54*, 11169.

[48] A. Ruzsinszky, J. P. Perdew, J. M. Tao, G. I. Csonka, J. M. Pitarke, *Phys. Rev. Lett.* **2012**, *109*, 233203.

[49] V. V. Gobre, A. Tkatchenko, *Nat. Commun.* **2013**, *4*, 2341.

[50] T. Bjorkman, A. Gulans, A. V. Krasheninnikov, R. M. Nieminen, *Phys. Rev. Lett.* **2012**, *108*, 235502.

[51] P. E. Blöchl, *Phys. Rev. B* **1994**, *50*, 17953.

[52] A. Gulans, M. J. Puska, R. M. Nieminen, *Phys. Rev. B* **2009**, *79*, 201105.